Citation: Molecular Therapy — Methods & Clinical Development (2016) **3,** 16080; doi:10.1038/mtm.2016.80
Official journal of the American Society of Gene & Cell Therapy

www.nature.com/mtm

ARTICLE

"Marker of Self" CD47 on lentiviral vectors decreases macrophage-mediated clearance and increases delivery to SIRPA-expressing lung carcinoma tumors

Nisha G Sosale[1], Irena I Ivanovska[1], Richard K Tsai[1], Joe Swift[1], Jake W Hsu[1], Cory M Alvey[2], Philip W Zoltick[3] and Dennis E Discher[1,2]

Lentiviruses infect many cell types and are now widely used for gene delivery *in vitro*, but *in vivo* uptake of these foreign vectors by macrophages is a limitation. Lentivectors are produced here from packaging cells that overexpress "Marker of Self" CD47, which inhibits macrophage uptake of cells when prophagocytic factors are also displayed. Single particle analyses show "hCD47-Lenti" display properly oriented human-CD47 for interactions with the macrophage's inhibitory receptor SIRPA. Macrophages derived from human and NOD/SCID/Il2rg$^{-/-}$ (NSG) mice show a SIRPA-dependent decrease in transduction, *i.e.*, transgene expression, by hCD47-Lenti compared to control Lenti. Consistent with known "Self" signaling pathways, macrophage transduction by control Lenti is decreased by drug inhibition of Myosin-II to the same levels as hCD47-Lenti. In contrast, human lung carcinoma cells express SIRPA and use it to enhance transduction by hCD47-Lenti- as illustrated by more efficient gene deletion using CRISPR/Cas9. Intravenous injection of hCD47-Lenti into NSG mice shows hCD47 prolongs circulation, unless a blocking anti-SIRPA is preinjected. *In vivo* transduction of spleen and liver macrophages also decreases for hCD47-Lenti while transduction of lung carcinoma xenografts increases. hCD47 could be useful when macrophage uptake is limiting on other viral vectors that are emerging in cancer treatments (*e.g.*, Measles glycoprotein-pseudotyped lentivectors) and also in targeting various SIRPA-expressing tumors such as glioblastomas.

Molecular Therapy — Methods & Clinical Development (2016) **3**, 16080; doi:10.1038/mtm.2016.80; published online 7 December 2016

INTRODUCTION

Uptake of viruses and all other types of particles by the mononuclear phagocyte system, particularly macrophages, is an extremely efficient process. Lentiviral vector (Lenti)[1–3] delivery of genes to *non*-phagocytic cells can be effective and useful *in vitro*, but *in vivo* viral vectors are predominantly cleared by mononuclear phagocyte system macrophages with the vast majority of a transgene expressed by macrophages in spleen, liver, and bone marrow.[4,5] Uptake by phagocytes of an enveloped virus is mediated in part, even in naive serum, by opsonins such as immunoglobulin and complement that can bind or physisorb to lentivectors during production in culture and postinjection.[6–10] Acute or chronic inflammatory responses initiated by vector components can occur after uptake,[11,12] and antibodies that result from adaptive immunity often enhance viral uptake *via* Fc receptors,[13–16] which are generally restricted to phagocytes. Reduction of viral clearance by the innate immune system has therefore been attempted by modification with synthetic polymers[17] analogous to "stealth" coatings on liposomes that delay deposition of opsonizing serum proteins which drive clearance (*e.g.*, Cullis *et al.*[18]). However, polymer brushes tend to sterically inhibit VSV-G and other envelope proteins used to target viruses to nonphagocytic cells for diverse therapies.[10,19,25]

CD47 is an integral membrane protein located on all human and mouse cells, and its immunoglobulin-like N-terminal domain is a ligand for an immunoinhibitory receptor SIRPA that is abundant on macrophages[26] and some nonphagocytic cells. Upon CD47 binding, SIRPA activates the phosphatase SHP-1 (ref. 27), which inhibits the cytoskeleton-intensive phagocytosis of cells and large particles that are opsonized by antibody and complement among other antagonistic factors.[28,29] By this pathway, CD47 acts as a "Marker of Self" as originally described when CD47-deficient red cells were injected into control mice and found to be rapidly cleared by splenic macrophages.[30] While marker of self capability has been examined in a variety of cell types and also synthetic beads whether such a signal would likewise function on a virus that is 100-fold smaller than a cell is unclear. CD47 is less effective at inhibiting uptake for rigid targets,[32] and viruses are much stiffer than nucleated mammalian cells and even more so than deformable red blood cells.[31] A viral capsid budding through a host membrane should in principle incorporate CD47 in the membrane envelope, but CD47 densities are low on normal cells.[28] We hypothesized that overexpression of full-length human CD47 (hCD47) on an otherwise standard virus-producing cell line would generate Lenti with sufficient hCD47 to specifically signal against macrophage uptake of these complex particles.

[1]Biophysical Engineering Labs, University of Pennsylvania, Philadelphia, Pennsylvania, USA; [2]Pharmacological Sciences Graduate Group, University of Pennsylvania, Pennsylvania, USA; [3]Children's Hospital of Philadelphia, Philadelphia, Pennsylvania, USA; Correspondence: DE Discher (discher@seas.upenn.edu)
Received 1 May 2016; accepted 6 October 2016

Following structural studies of CD47-Lenti, our functional studies *in vitro* assess uptake by phagocytic cells and by nonphagocytic cells. NOD/SCID/Il2rg$^{-/-}$ (NSG) mice are then used to assess *in vivo* whether hCD47-Lenti show enhanced circulation and gene delivery to lung cancer xenografts as NSG mice express a unique mouse variant of mSIRPA that binds human-CD47 (ref. 33) in contrast to other murine SIRPA variants that do not bind to human CD47 with comparable affinity.[34] NSG mice lack functional lymphocytes,[35] but have functional macrophages[36] so that the NSG model allows the focused study of macrophages in lentiviral vector clearance. On the other hand, SIRPA has long been reported to be expressed on cells other than immune cells,[27] and we discover here that targetable SIRPA is expressed at low levels on human lung cancer derived epithelial cells. Targeting of SIRPA could thus become useful for gene therapy of lung carcinoma,[37,38] perhaps even with systemic delivery that accesses multiple sites of disease. Since "Marker of Self" inhibition of liver clearance is less clear from past studies than splenic clearance, and because the liver is a desirable target for expression of transgenes such as coagulation factors,[39] we try to also clarify effects on Kupffer cells, which are the dominant liver macrophages.[40] Five independent experimental results *in vitro* and *in vivo* with human or mouse macrophages demonstrate "*anti-targeting*" of macrophages. The findings could be relevant to other viral vectors that are the basis for successful cancer treatments (*e.g.*, Measles glycoprotein pseudotyped lentivectors[41,42]) and perhaps to targeting other SIRPA-expressing tumors and tissues.

RESULTS

Virus display of "Marker of Self" CD47

Lentiviral vectors are often packaged within human-derived HEK 293T cells (e.g., Naldini *et al.*[43]), and transduction of this epithelial cell line with a human CD47-GFP construct shows the GFP signal is predominantly at the plasma membrane (Figure 1a). Immunostaining of fixed but nonpermeabilized cells with an antibody to hCD47's extracellular Ig domain further shows a maximum intensity at cell-cell junctions where the antibody can cross-bridge hCD47 between two membranes (Figure 1a). CD47-GFP on epithelial cells is highly mobile,[34] which should be conducive to integration into viral envelopes. Western blotting of "HEK CD47+" cells shows a 60 kDa band that is absent in control HEK 293T cells and is consistent with the CD47-GFP fusion protein (Figure 1b). Quantitation of GFP and anti-CD47 intensity across the cell membrane indicates high signal at the cell edge as compared to the center of the cell where the DNA-bound-Hoechst 3342 signal is maximum (Supplementary Figure S1a). Flow cytometry measurements of anti-CD47 intensity on the transduced cells indicate 15-fold higher CD47 density than on control cells (Supplementary Figure S1b). Mass spectrometry analyses of the "HEK CD47+" cells also detected three peptides from the human CD47 Ig domain (Supplementary Figure S1c) with a mean ion current that was also >>10-fold that of control cells (Supplementary Figure S1c). Accounting for cell surface areas, the small human red cell with ~25,000 molecules of hCD47 per cell[44] and the large HEK CD47+ cells are calculated to have similar hCD47 densities (Supplementary Figure S1d) that are well above the minimum level of CD47 density needed for inhibition of macrophage uptake based on studies of recombinant hCD47 Ig domain on opsonized beads.[45,46] Control HEK cell membranes have hCD47 densities below this minimum CD47 density so that standard Lenti particles that bud from conventional HEK cells are unlikely to signal "Self" with hCD47, whereas viruses that bud through the HEK CD47+ membranes can in principle display abundant hCD47 (Supplementary Figure S1d).

Lenti rich supernatants produced by HEK-CD47 cells transfected with standard plasmids were concentrated by ultracentrifugation and immobilized on coverslips pre-coated with anti-CD47 in order to image GFP+ particles. High-resolution total internal reflection fluorescence microscopy revealed fluorescent nano-particles (Figure 1c, Supplementary Figure S2a) whereas control Lenti were not fluorescent. Importantly, ~50% of GFP+ particles were also positive for acridine orange, which fluoresces red when bound to single-stranded RNA or DNA after permeating membranes (Figure 1c inset). The result is consistent with the ssRNA in lentivirus.[47]

Distributions of particle intensities were dominated by a single population (Supplementary Figure S2b, c) as were particle height distributions measured by atomic force microscopy, which give a ~120 nm peak (Supplementary Figure S2d, e) consistent with Lenti.[48–50] Immobilization of intact CD47-Lenti to glass coverslips was also observed only with antibody to hCD47's Ig domain and binding occurred in minutes, whereas anti-GFP and nonspecific antibody showed little to no immobilization of particles even after hours of incubation (Figure 1d). Anti-GFP showed ~10-fold less binding as compared to anti-CD47, which suggests this C-terminal epitope is within the lentiviral envelope as expected. Consistent with binding being a result of a CD47 anti-CD47 binding interaction, reducing the anti-CD47 concentration by 10-fold resulted in ~10-fold less binding. CD47's Ig domain is therefore oriented outward on the virus and available for binding SIRPA. Photobleaching of multiple fluorophores within a "spot" is used, for example, to determine the number of fluorescent nucleic acids incorporated by synthesis-based sequencing of single DNA molecules.[51] Photobleaching of GFP here occurred over several minutes with step-wise decreases in fluorescence (Figure 1e) consistent with bleaching single GFP molecules.[52] The quantization indicates at least ~12 molecules of CD47-GFP per particle. Approximately 12 CD47-GFP molecules or more per virus are expected for a ~120 nm diameter particle with CD47-GFP density similar to that on producer cells (291/μm^2 per Supplementary Figure S1d) whereas control particles from standard HEK cells are expected to display less than one CD47 molecule per virus—which is below what is needed to signal "Self" to macrophages (Supplementary Figure S1d).

To assess the ability of the CD47-lenti to present CD47 to a target cell a viral binding assay was performed between a murine-CD47-GFP+ lenti (mCD47-Lenti) and *human* HEK 293T cells (Figure 1f). Viral binding assays have been used previously to interrogate virus cell interactions.[53,54] The mCD47-Lenti was used in these experiments to distinguish lentivector presented CD47 apart from any endogenous human CD47 present on HEK cells. Flow cytometry was used to assess mCD47 and GFP display on the human HEK cells, and indicated the transfer of the mCD47-GFP fusion protein to the cell surface. This is consistent with the ability of the CD47-Lenti being able to display then transfer CD47 to the surface of a target cell.

Sucrose gradient ultracentrifugation of CD47-Lenti supernatants should enrich for the relatively dense capsid-containing virions from whole supernatants that also contain lighter cell debris, vesicles, and media components[55] (Supplementary Figure S3a). Such a separation was confirmed by an assay for functional titer of infectious virus in HEK 293T cells (Supplementary Figure S3b, c), SDS PAGE (sodium dodecyl sulfate polyacrylamide gel electrophoresis) analysis for viral capsid protein (p24) and serum albumin, as well as immunoblot analysis for CD47-GFP (anti-GFP (Supplementary Figure S3d) were performed. The virally delivered transgene in these and all studies below unless otherwise indicated is a CMV-promoter driven red fluorescent protein (RFP) variant DsRed.MST,[56,57] which allows for fluorescence quantitation of transduced cell numbers. Importantly gradient layers containing functional virus had both CD47-GFP and

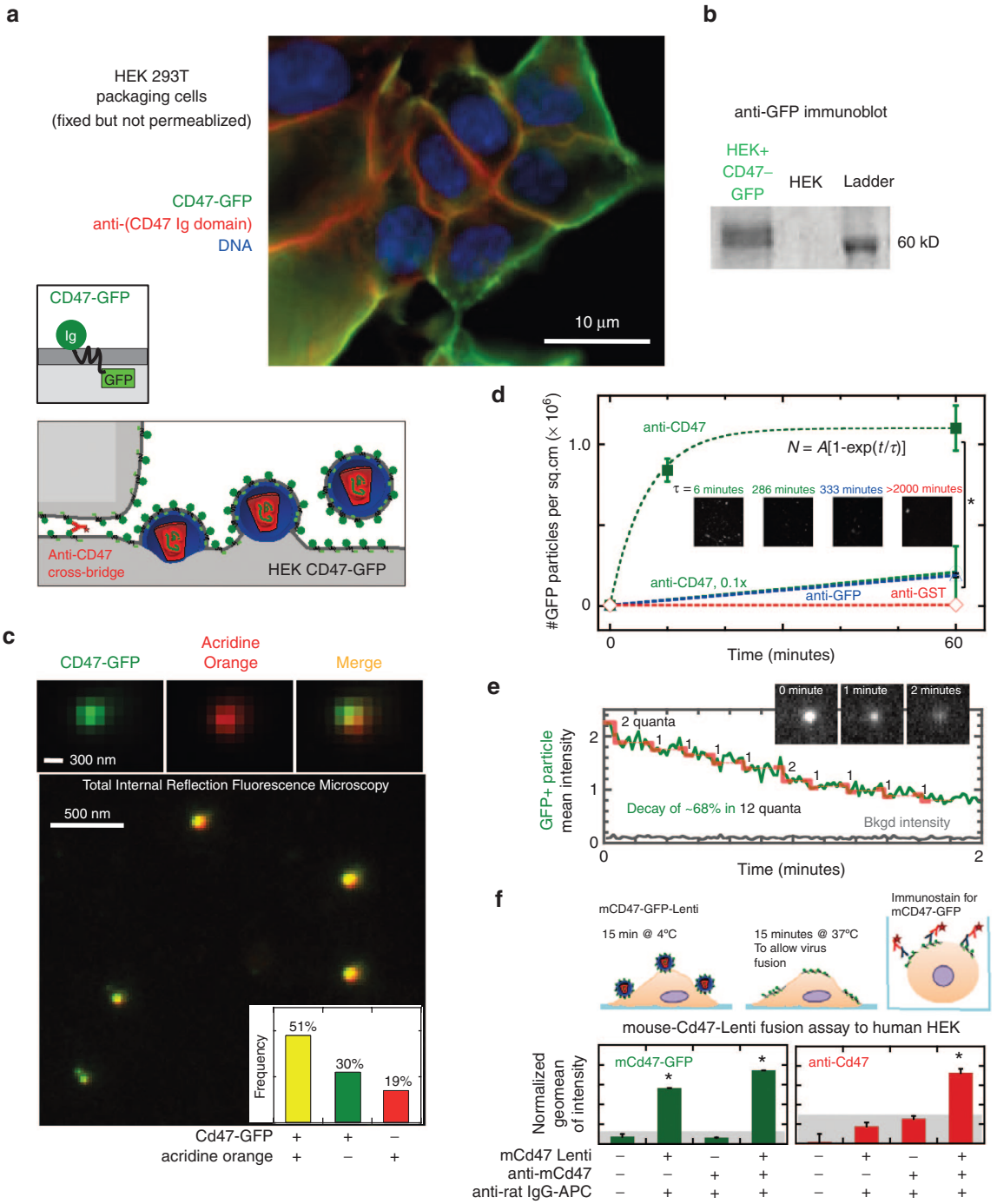

Figure 1 Lentivector display of "Marker of Self" CD47. (**a**) In HEK-CD47-GFP Producer cells the CD47-GFP (green) and anti-CD47 (red) signals are localized to the cell periphery, distinct from the nucleus (Hoechst, blue). CD47-GFP signal colocalizes with anti-CD47 immunostaining of the HEK-CD47-GFP cell membrane. Bivalent anti-CD47 localizes to cell-cell junctions. (**a**, schematic) Lentiviruses are enveloped viruses, where the viral capsid and genome self-assemble beneath the cell membrane and the assembled lentivirus then buds taking a piece of the cell membrane as the viral envelope (**a**, schematic). (**b**) Western blotting of HEK-CD47-GFP cells with an anti-GFP antibody confirms the presence of a 60 kDa protein, consistent in weight with a CD47-GFP fusion that is absent in control HEK cells. (**c**) HEK-CD47 lentiviral transfection supernatants were incubated with anti-CD47 coated coverslips, and adherent material was stained for acridine orange, which colocalized with the CD47-GFP fusion protein. The frequency of fluorescent and double positive particles was quantified (inset **c**). (**d**) CD47-Lenti binds IgG coated glass in an anti-CD47-dependent manner ($n \geq 3$, $P \leq 0.05$), dependence of binding kinetics on anti-CD47 is described by $rate = 1/\tau = a\,(\text{anti-CD47})^m$, m=1.8. (**e**) Lentiviral vectors were exposed to the TIRFM blue laser (~480 nm) for at least 2 minutes, and the CD47-GFP intensity of GFP+ particles over time was quantified, showing evidence of stepwise photobleaching (representative of $n = 3$). Red steps indicate quantal loss of 1–2 GFP fluorophores every ~10 seconds. (**f**) Flow cytometry was used to assess the fusion and binding of CD47-GFP+ lentivectors to human cells, which confirmed both that these vectors bind to the cell surface within 15 minutes of coincubation at 4*C and display the CD47-GFP fusion protein as detected by both GFP and anti-CD47 fluorescence.

p24 (Supplementary Figure S3e), while functional titer correlated over a ~500-fold range with p24 levels (Supplementary Figure S3f).

CD47 inhibition of macrophage transduction

To provide an *in vitro* model of a brief *in vivo* Lenti exposure as studied later, macrophage transduction by hCD47-Lenti versus control Lenti was assessed by *in vitro* infection (Figure 2a) of human-derived, PMA-differentiated THP-1 cells for just 1 hour. However, the lentivector to cell ratio (*i.e.*, multiplicity of infection (MOI)) was first quantified by the standard 72-hour infection of HEK 293T cells in the presence of the cationic polymer polybrene and serial dilutions of lentivector stocks. Polybrene enhances adsorption to a target cell independent of cellular receptors.[58] A rapid *in vitro* infection in just

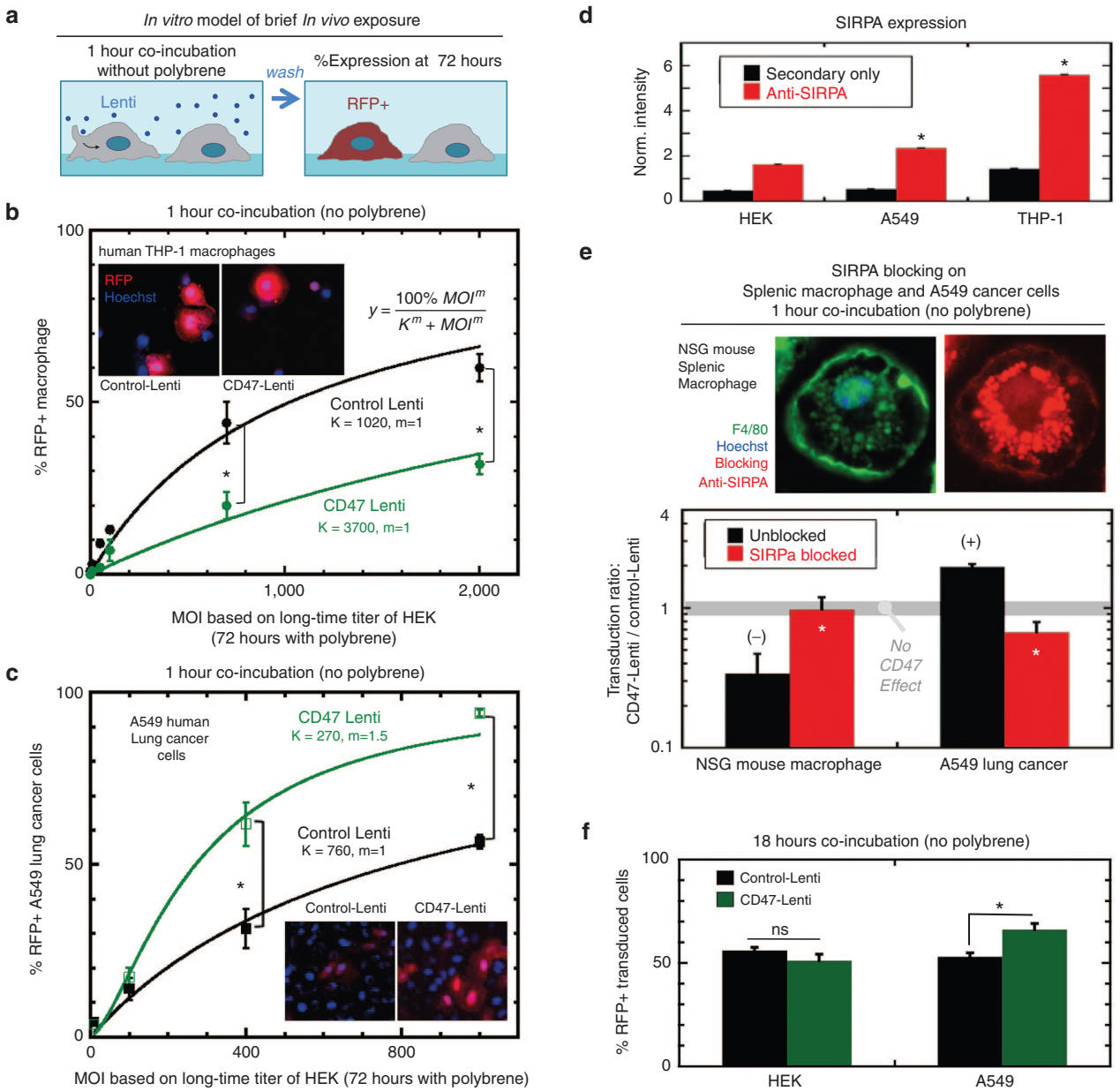

Figure 2 CD47 inhibition of macrophage transduction and enhancement of A549 transduction. CD47 and control Lentis encode the reporter transgene RFP variant DsRed.MST under the control of a CMV promoter. Either control or CD47 displaying Lenti were added to cells *in vitro* at a multiplicity of infection (MOI), or the ratio of number of lentivectors to number of cells, from 10 to 2,000. (**a**) Lentivectors were coincubated with cells for 1 hour followed by washing. (**b**) Seventy-two hours later, the percentage of transduced (%DsRed+) THP-1 macrophages and (**c**) A549 cancer epithelial cells was determined by RFP and Hoechst fluorescence quantitation. Both cell types showed a saturating response to MOI, and the transduction response was fit well by the Michaelis-Menten enzyme kinetics equation (%DsRed+=(100%*MOI/(K+MOI))), ($n \geq 3$, $P \leq 0.05$, $R^2 > 0.95$). (**d**) SIRPA expression on HEK 293T, A549 and THP-1, and THP-1+PMA cells was assessed by flow cytometry. The SIRPA signal is significantly higher for THP-1 than A549 cells, with both cell types presenting a signal that is significantly higher than background signal of secondary alone. In contrast, the HEK cells show a signal comparable to background signal, likely indicating HEK cells fail to present meaningful levels of SIRPA. (**e**) NSG murine splenic macrophage (F4/80+, SIRPA+) (MOI = 700) and A549 cells (MOI = 400) were pretreated or not with anti-muSIRPA or anti-huSIRPA (respectively) prior to infection. The ratio of CD47-Lenti transduction to control Lenti transduction was calculated for each condition. A ratio of 1 indicates equal transduction by the CD47- and control Lentis ($n \geq 3$, $P \leq 0.05$). (**f**) In addition to A549 cells, transduction of nonphagocytic HEK cells, that lack meaningful levels of SIRPA, was assessed (MOI = 50) and it was found that there is no significant difference in transduction by control versus CD47-Lenti in this cell line.

1 hour is therefore expected to require at least 72-fold more virus (multiplied by polybrene's effect) and is also relevant to receptor-mediated *in vivo* infection unlike the standard MOI assay using polybrene. Thus, in contrast to a standard *functional titer assay* for MOI, in the rapid *in vitro transduction assay* the lenti and target cells were coincubated for only 1 hour in the absence of polybrene (Figure 2a), in order to be a better predictive model for the *in vivo* delivery where most of the injected lentivector is cleared from circulation within hours rather than days.

At intermediate MOI, hCD47-Lenti transduced ~3-fold fewer macrophages than control Lenti (Figure 2b). Across the entire range of MOI's, standard hyperbolic dose–response curves fit very well, giving half-max transduction constants (*K*) of 3,700 versus 1,020 MOI units respectively for hCD47-Lenti versus control Lenti.

CD47 enhances of human lung cancer-derived epithelial cell transduction

In order to verify that our hCD47-Lenti and control Lenti were at least equally functional, the rapid 1-hour infection assays were done on a human lung cancer-derived epithelial cell line (A549). Gene therapy of lung carcinoma[37,38] might benefit if more virus is delivered to the cancer than to macrophages in the tumor or in the circulation. Surprisingly, hCD47-Lenti mediates threefold higher gene transfer than control Lenti (Figure 2c). Half-max transduction constants (*K*) respectively are 270 versus 760 in standard assay MOI units (for 72 hours transduction with polybrene of HEK cells). Importantly, the *K*'s for control Lenti transduction of A549s and THP-1s differ by only ~25% (760 versus 1,020 MOI), which is consistent with VSV-G-pseudotyped lentivectors being broadly infectious across cell types.[59] The 1-hour rapid infection gives a high MOI of 760 for A549 cells likely because of (i) a 72-fold greater requirement for virus than a 72-hour standard assay, and a (ii) a ~10-fold further increase with polybrene-mediated transduction in the standard assay. Neither 72-hour incubations nor polybrene are translatable to the *in vivo* studies below.

To explain the distinct results for hCD47-Lenti uptake, we measured the level of SIRPA protein on A549s and found it to be significant, consistent with other nonphagocytic cell types,[60] but also several fold lower than on the THP-1s and significantly higher than HEK 293T cells (Figure 2d). We therefore hypothesized that SIRPA functions as an inhibitory receptor in THP-1s but only as a docking receptor in A549s. The low level of measured SIRPA on HEK cells is approximately threefold that of the noise and thus SIRPA expression on HEK cells is unlikely to be meaningful (Figure 2d). Expression profiles for various lung cancer cell lines show SIRPA levels similar to the levels expected[61] and found for glioblastoma cell lines (Supplementary Figure S4).

SIRPA blocking was used to further test the first part of the above hypothesis, and in anticipation of *in vivo* studies below, transduction of NSG-derived splenic macrophages (F4/80+, SIRPA+) was examined (Figure 2e). After confirming that hCD47-Lenti transduced NSG-macrophages about threefold less effectively than control Lenti at the same MOI (Figure 2e, left black bar), which is consistent with the THP-1 results (Figure 2b), preblocking the NSG macrophages with anti-(mouse-SIRPA)[62] was shown to eliminate the difference in transduction between hCD47-Lenti and control Lenti and is plotted simply as a "Transduction Ratio" that becomes ~1 upon SIRPA blocking (Figure 2e, left red bar). Parallel experiments with the A549 cells used anti-(human-SIRPA) and showed that the higher transduction of these epithelial cells by hCD47-Lenti was eliminated by this function-blocking antibody (Figure 2e, right red bar). Thus with respect to CD47-Lenti interactions, SIRPA in these epithelial cells acts opposite to SIRPA in macrophages. Transduction of HEK cells, which express minimal SIRPA (Figure 2d), showed no significant effect of CD47 display on Lenti (Figure 2f), suggesting that the CD47-enhanced transduction of A549 cells depends on SIRPA as a docking receptor. The 18-hour coincubation time used here differs from the 1 hour incubation time used previously, but allows for a comparison of the ability of CD47 to transduce HEK versus A549 cells which differ in their levels of SIRPA display.

An additional transduction experiment was designed to test our estimations above that transduction would be more efficient for longer infection times (of 72 hours). We also sought to test whether CD47-Lenti can efficiently transduce A549 cells with a transgene other than RFP, and so CRISPR Cas9 was packaged with a guide-RNA that targets GFP. An A549 sub-line was made to stably express GFP as a fusion with Lamin-A, which in humans is a highly mutated gene that causes accelerated aging, muscular dystrophy, lipodystrophy, etc. For a given MOI, the CD47-Lenti transduced >50% more cells than Control Lenti (Figure 3). An advantage of CD47 display is predictably reduced at longer infection times because control Lenti will also eventually transduce all cells. Importantly, the longer infection time of 72 hours gave ~50% transduction with MOI ~ 10 compared to 1 hour infection requiring an MOI ~ 760 (Figure 2c). Polybrene should increase transduction further (~10-fold) but would over-ride CD47-mediated docking of Lenti to SIRPA.

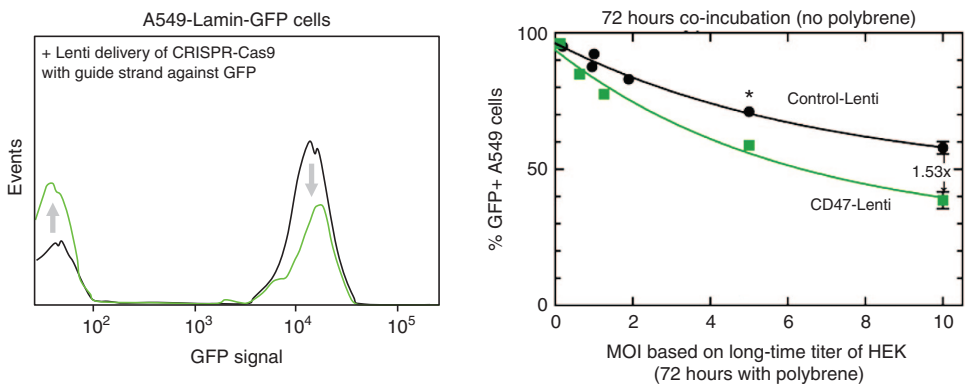

Figure 3 CRISPR-Cas9 gene deletion can be enhanced with CD47-Lenti for SIRPA expressing cells. A549 cells were transduced with either control or CD47-Lenti encoding a CRISPR Cas9 with guide strand targeting GFP in an already integrated GFP-lamin-A. GFP expression was assessed by flow cytometry (left), and both vectors resulted in >100-fold decrease in Lamin-A levels from a small %-age low/negative cells for GFP-lamin-A. The CD47-Lenti was able to deliver to 50% more cells than the control Lenti.

Myosin-II makes phagocytosis efficient unless inhibited by CD47 or drug

Expression profiles for uptake pathways within human and mouse macrophages versus A549 and HEK epithelial cells show that only macrophages express abundant receptors for immunoglobulin and complement (Figure 4a). These latter opsonizing factors deposit on particles even in naive serum during virus production in cultures and/or postinjection.[6–9] THP-1, A549, and HEK cells also express VSV-G receptors and proteins involved in clathrin-mediated endocytosis in lenti,63–65 which is likely used because (i) transduction of A549 cells remained significant while blocking SIRPA (Figure 2e), and (ii) transduction of macrophages occurs in spite of CD47-SIRPA inhibition of phagocytosis (Figure 2b,e). Downstream signaling to myosin-IIA (*MYH9*) in phagocytosis is distinct in making engulfment highly efficient[66] unless CD47-SIRPA engages to ultimately inhibit this motor.[28] As shown in our studies of phagocytosis of nanobeads,[46] the Myosin-II ATPase inhibitor blebbistatin should inhibit macrophage uptake similar to the effect of displaying CD47 (Figure 4a) while leaving uptake by other pathways intact.

THP-1 macrophages and A549 cells were pretreated for 1 hour with blebbistatin (5–50 µmol/l) and then control Lenti or hCD47-Lenti were added. The effect of blebbistatin on macrophage transduction by hCD47-lenti was not significant, which is consistent with Lenti-displayed-CD47 mediating myosin inhibition. However, transduction by the control Lenti decreased with high blebbistatin to that of hCD47-Lenti (Figure 4b). The half-max inhibition constant of ~5 µmol/l is fully consistent with inhibition of the Myosin-IIA ATPase,[67] and our earlier studies showed such results for phagocytosis of cell-sized objects correlated well with signaling to myosin-IIA, its localization to the synapse, and its overall abundance.[28,46] This indicates that the majority of transduction or gene delivery in macrophages is myosin dependent, consistent with phagocytic engulfment, while only a minor fraction of gene delivery is myosin-independent. Importantly, transduction of A549 cells by the control Lenti proved independent of myosin-II inhibition (Figure 4c). The control lenti was focused on here in order to examine blebbistatin-mediated myosin-inhibtion in the absence of CD47 effects. These results support the conclusions that Myosin-IIA contributes to the efficient uptake of Lentis by macrophages and that CD47 reduces macrophage uptake of Lentis by inhibiting Myosin-IIA. With non-phagocytic cells, CD47-Lenti uptake is independent of myosin-II, so that SIRPA acts not as an inhibitor but as an additional docking receptor for pathways additional to those normally used by VSV-G. While phagocytosis is made efficient by myosin activation,[66] VSV-G-LDLR mediated endocytosis is expected to be myosin-independent. The blebbistatin-inhibition results here are consistent with the majority of gene expression in macrophages being downstream of the myosin-dependent phagocytic uptake process. This further suggests that myosin-dependent phagocytosis is capable of resulting in successful transduction or transgene expression. While it is possible that inhibiting myosin-dependent phagocytosis might alter the distribution of uptake that is via phagocytosis versus via VSV-G-LDLR-mediated endocytosis, the results here indicate that inhibition of myosin results in a decrease in gene transfer to THP-1 macrophages.

CD47-Lenti enhances *in vivo* circulation unless SIRPA is blocked

To determine the impact of CD47 display on *in vivo* circulation of lentivirus, either a control or hCD47-Lenti were injected into the tail veins of NSG mice, and the blood was periodically sampled for functional titer assay in HEK 293T cultures (Figure 5a; Supplementary Figure S5a). A range of relevant doses were examined *in vivo* (3×10^8 to 1×10^9, Supplementary Figure S5b).[5,11] Both control and hCD47-Lenti were progressively cleared from the bloodstream (Figure 5a), but the control Lenti was cleared more rapidly so that the persistence ratio (circulating hCD47-Lenti)/(control Lenti) increased with time (Figure 5b). At 10 minutes postinjection, this ratio favored hCD47-Lenti by just threefold, but by 45 minutes the advantage of hCD47-Lenti increased to nearly 10-fold relative to control lentivectors and independently of vector dose (Supplementary Figure S5b), and is significantly higher at both 45 minutes and 24 hours postinjection as compared to 10 minutes ($P = 0.01$ and $P = 0.05$ respectively). While this ratio remains high up to 24 hours postinjection, decreasing titers add uncertainty to subsequent ratios.

Fitting just the initial 45 minutes of ratio data with an exponential not only provides a good fit but also yields a fitting constant T = 15 minutes postinjection, which is the time at which hCD47-displaying Lenti are twofold more abundant than control Lenti (Supplementary Figure S5c). This persistence ratio doubling time agrees well with the T ≈ 20–30 minutes obtained for the CD47-conferred advantages in circulation of highly opsonized mouse red cells and also of highly opsonized nanobeads.[46] Our previous nanobead results (also in NSG mice) proved statistically the same when two colors of particles were injected in the same mouse for particle ratio analyses as when a single particle type was analyzed as here, and analyses once again began 10 minutes after injection to ensure good mixing (for retro-orbital blood sampling). Circulation results for *unopsonized* mouse and human red cells[30,61] yield T ~ 10 hours in similar analyses (Supplementary Figure S5c), which means the advantage of CD47 is slow to manifest for unopsonized entities in circulation. The comparison is therefore again consistent with virus becoming opsonized[8] and driving macrophage-mediated clearance.[6,15] The comparison also indicates that CD47 delays opsonization-driven clearance *in vivo*.

The lentivector titer in circulation 45 minutes after injection relative to that at 10 minutes defines for each mouse a viral kinetics ratio (VKR) that succinctly characterizes the effect of blocking *in vivo* with anti-mSIRPA. Anti-mSIRPA blocks macrophage interactions with CD47 not only *in vitro* (Figure 2e) but also *in vivo* where it binds NSG macrophages.[46] Preinjecting this antibody in NSG mice indeed decreases the VKR significantly for CD47-Lenti (Figure 5c). CD47-Lenti's antibody-blocked VKR is also statistically similar to that of control Lenti. The enhanced *in vivo* circulation of CD47-Lenti is therefore due to a CD47-SIRPA interaction.

In vivo transgenes: decreased in macrophages, increased in tumor cells

CD47-inhibited clearance of cells has primarily been attributed to impeding uptake by splenic red pulp macrophages.[30] Spleens of NSG mice were therefore isolated 5 days after injection in order to allow sufficient time for expression of the transgene, and then the spleens were dissociated into single cell suspensions for identification of transduced macrophages (positive for F4/80, known also as Emr1, and Sirpa, Figure 2e). Mice injected with CD47-Lenti showed nearly twofold fewer DsRed+ splenic macrophages relative to mice injected with control Lenti (Figure 6a). This is quantitatively consistent with the two- to threefold enhancement of circulating CD47-Lenti (Figure 5b,c).

NSG mouse livers were sectioned. Confocal imaging of immunofluorescence show F4/80+ cells with a reticulated morphology consistent with Kupffer cell macrophages (Supplementary Figure S6a) and also show an abundance of mouse-CD47+ cells with round mor-

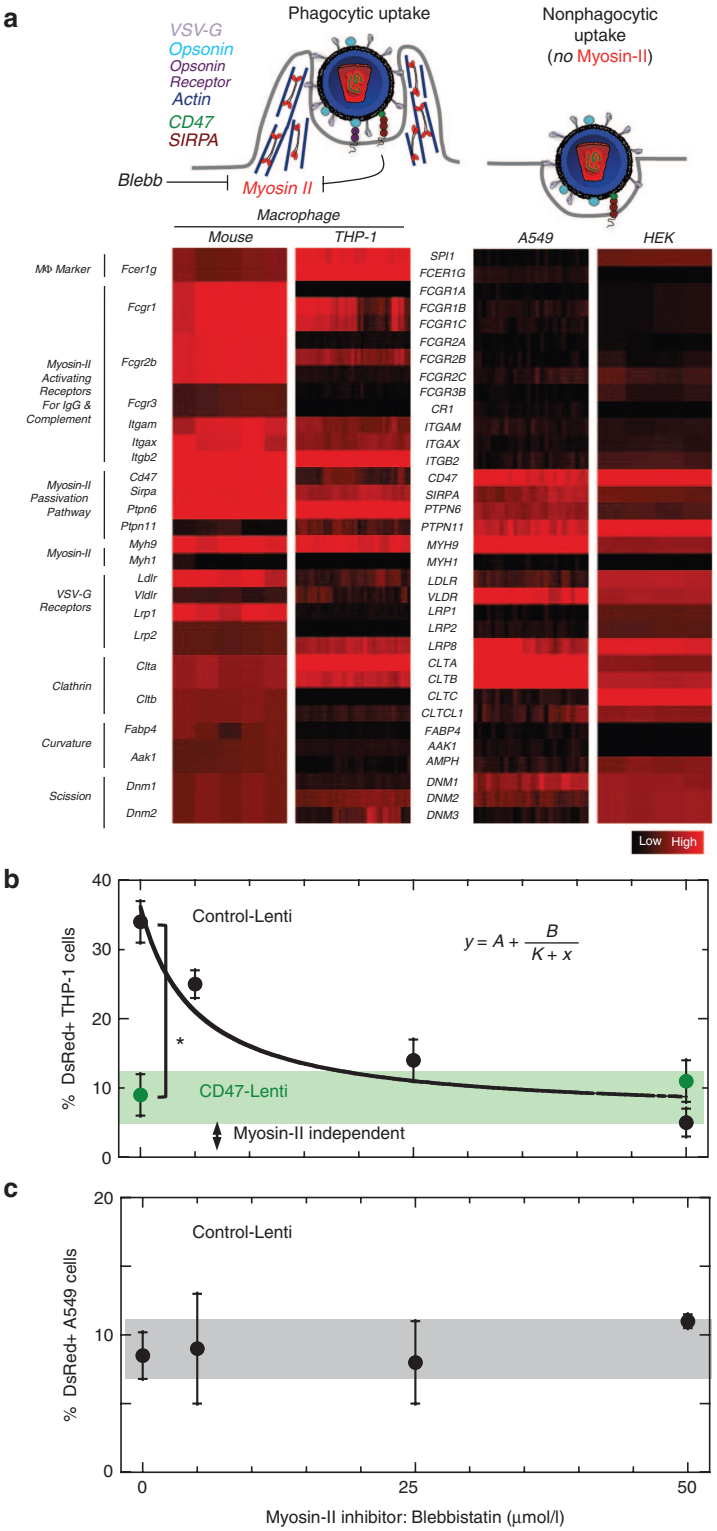

Figure 4 Mechanism of Inhibition and Enhancement. (**a**) Lenti CD47 display is expected to inhibit uptake by macrophage via binding to SIRPA, which leads to deactivation of proteins involved in macrophage uptake including the Myosin-II motor. Myosin-II can also be inhibited by Blebbistatin. Expression profiles for uptake pathways within human and mouse macrophages versus A549 epithelial cells were plotted where black indicates a minimum value and red a maximum value. Gene expression values: {(minimum, middle, maximum, %over-mid, %under-mid): murine MΦ (0,9.2,10.5,2.1,18.9), human MΦ (2,6.1,7.7,0,19.7), A549 (1.7,2.2,3.6,0.2,0.4) HEK (3.2, 11.4, 5.2, 2.5 11.4, 5.2)}. Genes include those encoding activating receptors for antibody and complement, proteins of the myosin-II passivation pathway, and myosin-II motors. *Myh1/MYH1* is skeletal muscle myosin and serves as a negative control as it is not expressed in nonmuscle tissues. The A549 lung epithelial cell line lacks activating receptors but expresses SIRPA. (**b**) Macrophages were pre-treated with myosin-II inhibitor blebbistatin (5–50 μmol/l) and then transduced with either control or CD47-Lenti ($n \geq 3$, $P \leq 0.05$) (MOI = 700). The control Lenti macrophage transduction response to blebbistatin concentration fit well to a standard inhibition curve ($y = A + B/(K_i + x)$, $R^2 > 0.98$), with A = 6%, B = 225% μmol/l, and, $K_i = 7.8$ μmol/l. (**c**) A549 cells were pretreated with drug for 1 hour prior to transduction with control Lenti (MOI = 270). Transduction shows no significant effect of the myosin-II inhibitor.

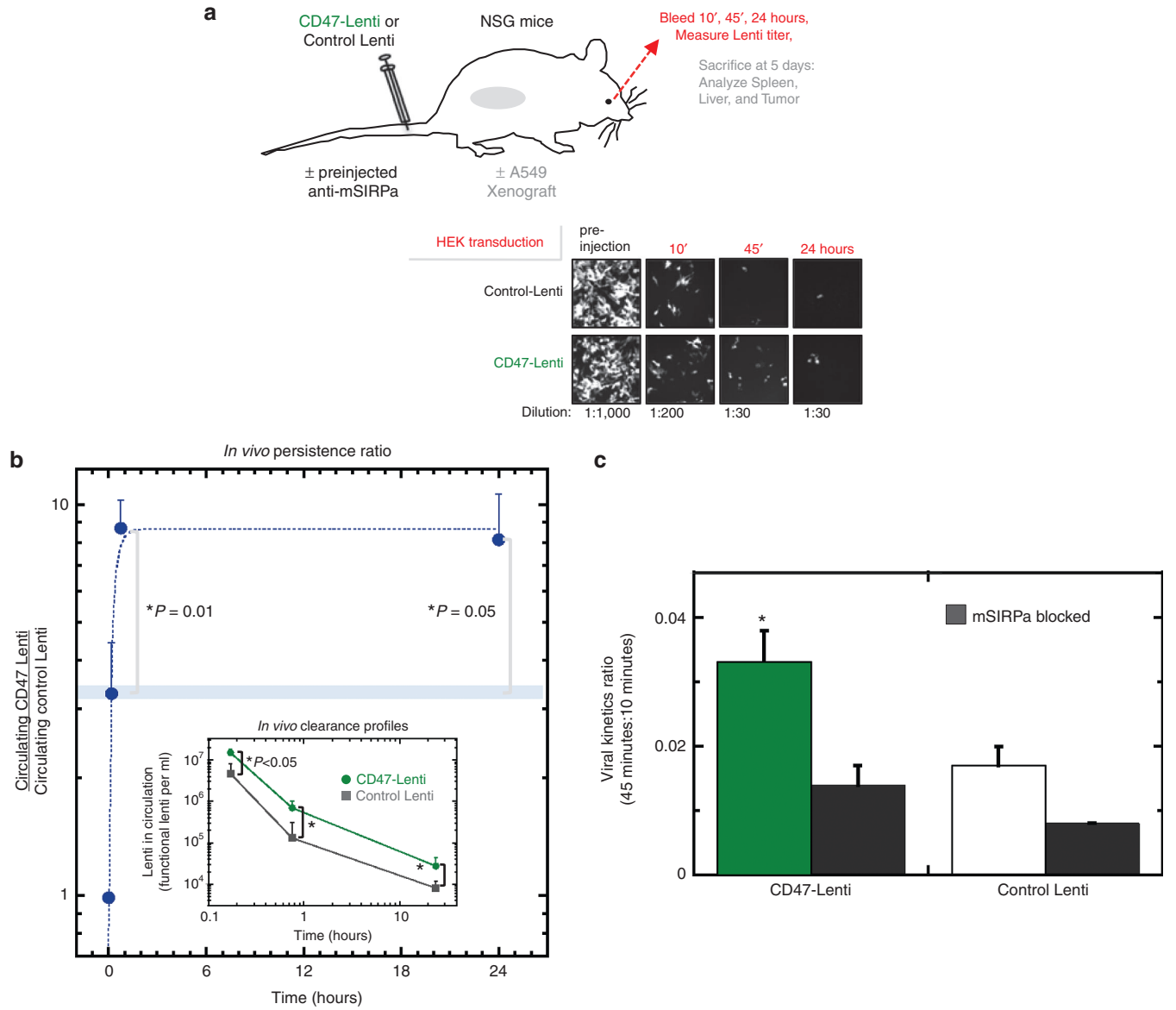

Figure 5 CD47-Lenti shows enhanced *in vivo* circulation. (**a**) CD47 or control Lentis were injected *via* tail vein into NSG mice, and 10 minutes, 45 minutes, and 24 hours bleeds were analyzed for Lenti concentration by a functional titer assay. Representative images of the functional titer assay show a higher number of RFP+ HEK cells with the CD47-Lenti blood samples than the control-Lenti blood samples. (**b**) Either control or CD47-Lenti (1×10^9) were injected via the tail vein to NSG mice. The persistence ratio, the relative concentration of CD47-Lenti relative to control Lenti, was quantified (At 10 and 45 minutes postinjection, $n = 13$; at 24 hours postinjection, $n = 6$). Both control and CD47-Lenti were cleared from the blood stream, with the control Lenti being cleared more rapidly (**b**, lower inset, $^*P \leq 0.05$). By 45 minutes postinjection, CD47-Lenti are nearly 10-fold more abundant in circulation than control Lenti. The difference in the persistence ratio at 45 minutes as compared to the persistence ratio at 10 minutes is statistically significant ($P = 0.01$). The difference in the persistence ratio at 24 hours as compared to the persistence ratio at 10 minutes is statistically significant ($P = 0.05$). (**c**) The virus kinetics ratio (VKR), or the ratio of virus remaining in circulation at 45 minutes relative to that at 10 minutes, was quantified and gives another measure of the persistence in circulation of the lentivector. Further, SIRPA was blocked *in vivo* with an anti-SIRPA mAb against mouse SIRPA, or not, prior to injection of Lenti ($n \geq 4$ unless indicated). The VKR for CD47-Lenti was significantly higher than the VKR for CD47-Lenti with mSIRPA blocking ($P = 0.03$). There was no significant difference between the VKR for CD47-Lenti with SIRPA blocking condition as compared to the control-Lenti ($P = 0.11$).

phologies consistent with hepatocytes (Supplementary Figure S6b). Both control Lenti and CD47-Lenti transduced Kupffer cells and hepatocytes (Supplementary Figure S6c, d), but quantitation indicated twofold fewer DsRed+ Kupffer cells for CD47-Lenti (Figure 6b). To our knowledge, CD47-inhibited clearance has not been reported for Kupffer cells; but these macrophages can derive from bone marrow,[40] and phagocytosis of bone marrow-derived macrophages is certainly inhibited by the CD47 pathway.[30] Expression profiles of liver were therefore analyzed and indeed provide evidence of *Emr1*-expressing cells (*i.e.*, macrophages) with abundant *SIRPA* and *SHP1* (*Ptpn6*) (Supplementary Figure S6e). Transduction appeared restricted to macrophages rather than parenchymal cells (Supplementary Figure S6f). In light of the similar twofold decrease in transduction of Kupffer cells and splenic macrophages with CD47-Lenti here, a similar inhibitory pathway seems likely in both liver and spleen.

A more persistent circulation and reduced uptake by macrophages with the CD47-Lenti suggests that the greater abundance of these novel lentivectors in blood may allow for greater transduction of other accessible cells relative to control Lenti. Advances in gene

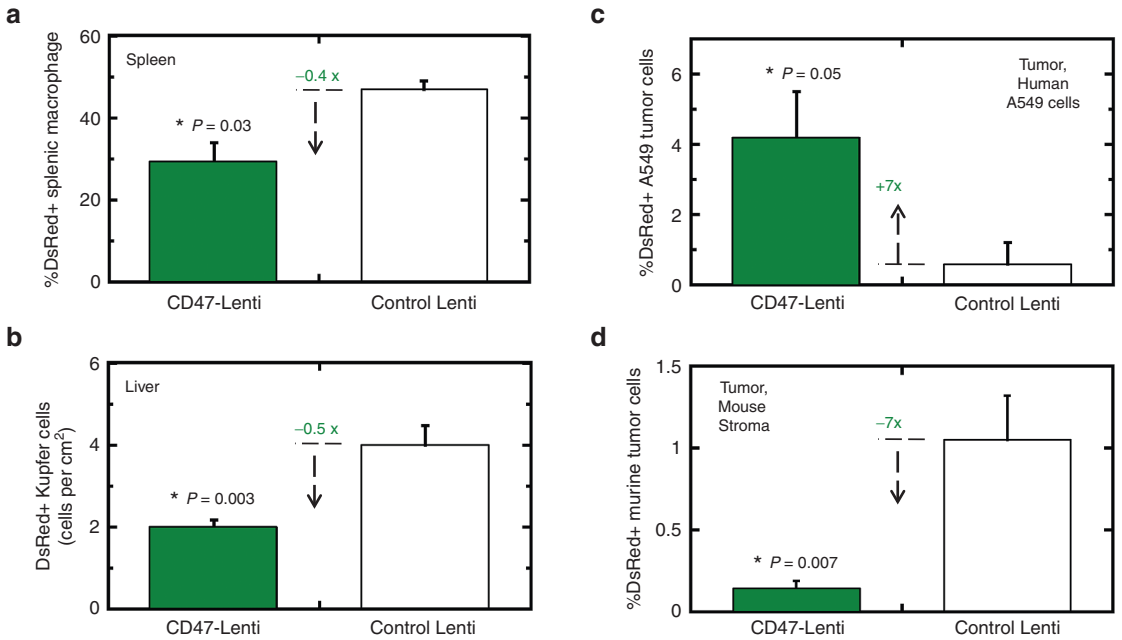

Figure 6 CD47 inhibits DsRed expression by macrophages *in vivo* and enhances DsRed expression in human tumor cells. (**a**) 1×10^9 CD47- or control Lenti were injected via tail-vein. Spleens were mechanically dissociated 5 days postinjection. Splenic macrophage were identified by F4/80 immunostaining, and analyzed for DsRed transgene expression by flow cytometry. CD47-Lenti injected spleens showed decreased splenic macrophage transduction. (**b**) 1×10^9 CD47- or control Lenti were injected via tail-vein. 5 days postinjection livers were isolated. Tissue sections were imaged for RFP expression by confocal microscopy. Cells that were consistent with Kupffer cell morphology (Supplementary Figure S5a–d) and positive for RFP expression were quantified. (**c**) CD47- or control Lenti were injected via tail-vein to A549 xenograft-tumor bearing NSG mice, and 4 days postinjection tumors were isolated and analyzed for RFP transgene expression where CD47-Lenti mediated significantly higher transgene expression. For all, $n \geq 6$ unless indicated; $P \leq 0.05$. (**d**) Analysis of the huCD47-neg, muSIRPA-neg cells in the tumor indicated that CD47-lenti showed lower percent transduction of this mouse tumor stroma cell subset.

therapy show promise for treatment of lung cancer,[36,37] and solid tumors tend to be leaky to many types of circulating particles;[68–70] so, A549 xenografts in NSG mice were established and mice were tail-vein injected with the Lentis. After several days to allow for transgene expression, the xenografted tumors were removed, disaggregated, and cells were analyzed by flow cytometry (Supplementary Figure S6g). The A549-identified population showed on average ~7-fold more transgene-positive cells in mice injected with CD47-Lenti versus control Lenti (Figure 6c). We had found with the same xenograft model that CD47-nanobeads loaded with near-infrared dyes localized to the tumors three- to fivefold more so than nanobeads without CD47 (ref. 46). The result here is statistically similar. These model tumors are ~40–50% A549 cells and ~2–3% tumor associated macrophages,[80] but only ~5% of A549 cells were transduced by CD47-Lenti, probably because particles as large as lentiviruses (~100 nm) rarely permeate deeply into tumors.[71] Transduction of mouse stromal cells in the tumor (huCD47-neg, muSIRPA-neg) decreased significantly with CD47-Lenti (Figure 6d), but detectable signal indicates some transduction of non-macrophage cell types in tumors (*e.g.*, cancer associated fibroblasts). The CD47-Lenti results *in vivo* are thus consistent with increased circulation, decreased uptake by macrophages, and increased transduction of accessible human tumor cells displaying SIRPA.

DISCUSSION

Attachment of recombinant human-CD47's immunoglobulin domain to polystyrene nano-beads that were IgG-opsonized was found in our recent studies to be sufficient to repress macrophage uptake *in vitro* and *in vivo*.[46] SIRPα on macrophages acts via SHP1 phosphatase (PTPN6) as an inhibitory receptor,[46] but lentiviruses are far more complex than polystyrene beads and SIRPα on other cell types might not be inhibitory. The HIV-1 derived vector has an inner core composed of the matrix, nucleocapsid, and capsid (p24) proteins, with the latter assembling into a "fullerene cone" lattice.[58] Since the lipid-based envelope derives from host cells, current methods of enhancing delivery of lentivectors have rightly focused on display of envelope proteins that can enhance uptake[19,22] and gene expression within specific target cells.[36] Biodistribution studies show that lentiviruses are nonetheless taken up into macrophage-rich tissues[4] with gene expression preferentially found in macrophages.[36] Such uptake could in principle promote inflammation and challenge long-term transgene expression.

Macrophage uptake of viruses is likely to be diverse and distinct in terms of molecular mechanisms, but these professional phagocytes (which means eating cells) should be highly efficient at uptake compared to nonphagocytic cell types (*e.g.*, A549 cancer cells). Myosin-II activation indeed makes uptake efficient by macrophages for particles[46] as well as Lenti (see transgene expression for control Lenti in Figure 4b), but myosin-II is not activated in the less efficient uptake by nonphagocytic cell types (based on transgene expression in Figure 4c). There is certainly more to understand about uptake into phagosomes versus endosomes and ultimate transgene expression, but the consistency with past uptake studies of Lenti-sized synthetic particles suggests uptake is simply proportional to transgene expression. Thus, when myosin-II in macrophages is inhibited—such as when CD47 on a Lenti engages SIRPα on a macrophage, uptake is reduced and so is transgene expression.

Biodistributions of virus in antibody-free mice show a large shift from blood and other organs to spleen after just 30 minutes of pretreatment with naive serum, implicating "natural" IgM antibodies

but also perhaps IgG and IgA.[6] Complement in naive serum likewise deposits on virus.[7,8,72] Infection of phagocytic cells by HIV is enhanced with virus-specific antibodies,[15] and fetal bovine serum (FBS) that is commonly used in lentivector preparations as here can contain virus-directed immunoglobulins.[73] Liver and spleen macrophages express receptors for immunoglobulin and complement (Figure 4a; Supplementary Figure S6e), and both liver and spleen uptake of red cells is also clearly enhanced by opsonization of red cells.[74] Intravital imaging of liver has revealed the uptake of opsonized cells into Kupffer cells (F4/80+, Cd11b^{hi}),[75] and in the spleen, red pulp and marginal zone macrophages express functional receptors for antibody.[76] Splenic macrophages as well as bone marrow-derived macrophages are clearly inhibited by CD47 on cells,[28,30,77] and the findings here (Figure 6b) suggest that lentis which bud through cell membranes rich in hCD47 also have the ability to inhibit uptake by liver macrophages. This conclusion is important because there is otherwise little evidence that CD47 can inhibit uptake by liver macrophages and because the liver is a desirable target for expression of transgenes such as coagulation factors.[43]

The results here may have implications for the role of CD47 display in enveloped virus uptake. CD47 is expressed on all cell types, including leukocytes that are HIV-susceptible. HIV particles that bud from such cells might therefore display some CD47 on their envelope and thereby impact infection. Although results here suggest that HEK 293T producer cells would normally need to overexpress CD47 (Figure 1), leukocyte progenitors can sometimes increase their CD47 levels.[78] Moreover, a poxvirus encodes what has been claimed to be a CD47 ortholog that causes a more severe pathology than virus lacking the protein[79] presumably due to reduced activity of phagocytic cells, although relevance to CD47 remains controversial.[80] Decreased macrophage uptake has the potential to reduce immune responses downstream of myeloid cell uptake of Lentis,[11,12] and CD47 seems to modulate inflammatory response and induction of adaptive immunity.[71] While protein display by phagocytosed cells can affect the efficiency of antigen presentation,[81] any effect of CD47 on antigen processing and presentation following viral infection requires further study.

Past studies of CD47 have largely focused on interactions involving animal cells much larger than viruses, but the findings here perhaps deepen the current understanding of macrophage uptake processes and CD47-SIRPA inhibition at a very small scale. Moreover, CD47-Lenti may prove useful for gene therapy by this receptor-specific "*anti-targeting*" approach. Furthermore, since we find that CD47 is similarly low in abundance on these Lenti (~7–70 molecules) as gp120 on HIV-1 (~7–70 molecules)[82,83] and far lower than VSV-G on wild-type VSV (~600 molecules/um^2),[84] more CD47 might be displayed on CD47-Lenti and could help prolong circulation of any CD47^{low} particles. Nonetheless, moderate CD47 densities allow its display to be combined with receptor-specific targeting to diseased cells.[21,23,24] VSV-G-pseudotyped lentiviral vectors were the focus of the work here as they can transduce a wide range of cell types, stably integrate the gene of interest, and are enveloped viruses and therefore amenable to the CD47-overexpressing packing cell line method used here. The hCD47-HEK 293T producer cells might also be used to increase CD47 display on Measles glycoprotein-pseudotyped lentiviral vectors that are the basis for successful treatments.[41,42] Measles glycoprotein receptors SLAM and CD46 (ref. 85) are expressed on endothelial and epithelial cells as well as tissue macrophages in a number of tissues.[86] Like VSV-G, the Measles glycoprotein can be expected to mediate transduction of both macrophage and nonmacrophage cells so that CD47 on measles glycoprotein-pseudoptyped Lenti could reduce gene transfer to and expression in macrophages and act as a docking receptor for SIRPA displaying epithelial cells. In addition to lung cancers per the model here, SIRPA could be useful as a docking receptor for SIRPA-displaying cancers including glioblastomas (Supplementary Figure S4).

MATERIALS AND METHODS

Reagents, DNA constructs, cell lines, and standard methods are described in Supplementary Materials and Methods.

Generation of HEK-CD47-GFP producer cell line

HEK 293T cells (ATCC, Manassas, VA) were transduced with a lentivector encoding CD47-GFP and puromycin resistance transgenes. The CD47-GFP fusion has been previously described.[34] Lentiviral transduction was followed by puromycin (ThermoFisher, Bartlesville, OK) selection for 3 weeks. To produce the *CD47-Lenti,* the HEK CD47-GFP cells were transfected using standard methods.

Functional titer of concentrated lentiviral stocks

Lentiviral vector stocks were quantified for functional viral particles by a functional titer assay of HEK 293T cells. Serial dilutions of lentiviral vector stocks were prepared and added to HEK cells pretreated with DMEM (ThermoFisher) supplemented with Polybrene (8 µg/ml; Sigma-Aldrich, Milwaukee, WI). Exactly 72 hours postaddition of lenti, DsRed+ cells were quantified by fluorescence microscopy.

In vitro transductions

Cells were plated at 1E4 cell/cm^2. Lentis were added at an MOI from 10 to 2,000 where MOI (multiplicity of infection) is the ratio of the number of lentivectors to number of cells. Lentivector number was determined by a functional titer assay of HEK 293T cells (transducing units). Macrophages (THP1; ATCC) and lentivector were coincubated for 1 hour, unless otherwise specified. Seventy-two hours post-transduction, cells were assayed for reporter gene expression by fluorescence microscopy. Total cell number was determined by DNA stain (Hoechst 33342 Invitrogen, Bartlesville, OK). Human SIRPA was blocked with anti-human SIRPA (clone SE7C2; Santa Cruz; Dallas, TX), and mouse SIRPA was blocked with anti-(mouse-SIRPA) (clone P84; BD Biosciences, San Jose, CA). Where indicated, cells were pretreated with Blebbistatin (5–50 µmol/l; Sigma-Aldrich) for 1 hour prior to transduction.

In vivo injections and sampling

3×10^8 to 1×10^9 Lentis were injected via tail vein into NSG mice (Jackson Laboratory, Bar Harbor, ME). Blood was sampled via retro-orbital bleed at 10 minutes, 45 minutes, and 24 hours postinjection and analyzed by functional titer (Supplementary Methods). Four to five days postinjection, spleen, liver, and tumors were collected for immunohistochemistry analysis, or flow cytometry analysis of reporter gene expression. Hundred micrograms of anti-mSIRPA (P84) were preinjected 30 minutes prior to injection of lentivector for *in vivo* mSIRPA blocking studies.

In vivo injection and sampling

3×10^8 to 1×10^9 lentiviral particles were injected via teil vein to NSG mice. Blood samples were taken by orbital bleed at 10 and 45 minutes postlentiviral injection, and by cardiac puncture at 24 hours postinjection. Hundred micrograms of anti-mSIRPA (P84) were preinjected 30 minutes prior to injection of lentivector for *in vivo* mSIRPA blocking studies.

In vivo Lenti circulation functional titer

One day prior to blood sampling, HEK cells were plated in 24-well tissue culture plates. On the day of blood sampling, the HEK medium was replaced with polybrene containing DMEM medium+FBS (ThermoFisher). Four dilutions of each of the blood samples were prepared. Approximately 100 µl of each dilution was added to a well of the 24-well plate in triplicate. The cells and lentiviral containing blood sample were coincubated for 72 hours. At 72 hours postaddition, each well was examined using a fluorescent microscope for RFP expression. Wells that showed RFP expression that was in a

countable range (distinct RFP-positive cells) were imaged, with 30 images taken of each well. Images were quantified for the number of RFP+ cells per field of view using ImageJ (public domain Java image processing program; National Institutes of Health). The number of RFP+ cells was calculated based on micrometer measurement of the field of view and the vendor reported dimensions of the culture plate. The concentration of lentiviral vector in the blood sample was calculated from the calculated number of RFP+ cells and the volume of blood added to each well, where it was assumed that one RFP+ cell correlates with one functional lentiviral vector. Using this method, the concentration of lentiviral vector in the bloodstream was determined for each mouse at each time point.

Statistical analysis

Using Excel, the geomean and standard error of vector concentrations was taken for each vector-type (control-Lenti, CD47-Lenti) at each time point (10 minutes, 45 minutes, 24 hours). At each time point, the persistence ratio (PR) was calculated as the quotient of the CD47-Lenti geomean of lenti-vector concentrations relative to the Control-Lenti geomean of lentivector concentration.

$$PR = \frac{[CD47\_Lenti]}{[Control\_Lenti]}$$

The standard error was propagated for the ratio:

$$\frac{\sigma_{PR}}{PR} = \sqrt{\left(\frac{\sigma_{cd47-Lenti}}{[CD47\_lenti]}\right)^2 + \left(\frac{\sigma_{Control-Lenti}}{[ContoI\_lenti]}\right)^2}$$

For 10 and 45 minutes, n_CD47 = 7, and n_control = 6. At the 24-hour time point, n_CD47 = 3, and n_control=3 as some samples were to dilute by 24 hours postinjection to be quantified by the functional titer assay. An unpaired *t*-test was used to compare the PR at 45 minutes to the PR at 10 minutes, and the PR at 24 hours to the PR at ten minutes. The *P* values were corrected for multiple testing using the Benjamani Hochberg procedure.[87]

Calculation and analysis of the viral kinetics ratio

The geometric mean and standard deviation of functional titers at 45 and 10 minutes were calculated for four conditions: CD47-Lenti, CD47-Lenti with a mSIRPA blocking preinjection, control-Lenti, and control-Lenti with a mSIRPA blocking pre-injection. The ratio of the geomean of functional titer at 45 minutes to that at 10 minutes was calculated for each condition. We applied propagation of error to estimate the standard deviation for the ratio. To test for differences between VKRs for unblocked versus blocked CD47-Lenti and unblocked CD47-Lenti groups, we used the unpaired *t*-test.

CONFLICT OF INTEREST

The authors declared no conflict of interest.

ACKNOWLEDGMENTS

This work was supported by the National Institutes of Health, National Cancer Institute (grant U54-CA193417), National Heart, Lung, and Blood Institute (grant R01-HL124106), National Institute of Biomedical Imaging and Bioengineering (grant R01-EB007049), National Institute of Diabetes and Digestive and Kidney Diseases (grants P01-DK032094 and P30-DK090969), National Center for Advancing Translational Sciences (grant 8UL1TR000003); the National Science Foundation (Materials Research Science and Engineering Center and Nano Science and Engineering Center-Nano Bio Interface Center), and an International Research Training Group grant 1524.

REFERENCES

1. Consiglio, A, Gritti, A, Dolcetta, D, Follenzi, A, Bordignon, C, Gage, FH *et al.* (2004). Robust *in vivo* gene transfer into adult mammalian neural stem cells by lentiviral vectors. *Proc Natl Acad Sci USA* **101**: 14835–14840.
2. Worsham, DN, Schuesler, T, von Kalle, C and Pan, D (2006). *In vivo* gene transfer into adult stem cells in unconditioned mice by in situ delivery of a lentiviral vector. *Mol Ther* **14**: 514–524.
3. Lee, HJ, Lee, YS, Kim, HS, Kim, YK, Kim, JH, Jeon, SH *et al.* (2009). Retronectin enhances lentivirus-mediated gene delivery into hematopoietic progenitor cells. *Biologicals* **37**: 203–209.
4. Pan, D, Gunther, R, Duan, W, Wendell, S, Kaemmerer, W, Kafri, T *et al.* (2002). Biodistribution and toxicity studies of VSVG-pseudotyped lentiviral vector after intravenous administration in mice with the observation of *in vivo* transduction of bone marrow. *Mol Ther* **6**: 19–29.
5. Follenzi, A, Sabatino, G, Lombardo, A, Boccaccio, C and Naldini, L (2002). Efficient gene delivery and targeted expression to hepatocytes *in vivo* by improved lentiviral vectors. *Hum Gene Ther* **13**: 243–260.
6. Ochsenbein, AF, Fehr, T, Lutz, C, Suter, M, Brombacher, F, Hengartner, H *et al.* (1999). Control of early viral and bacterial distribution and disease by natural antibodies. *Science* **286**: 2156–2159.
7. Beebe, DP and Cooper, NR (1981). Neutralization of vesicular stomatitis virus (VSV) by human complement requires a natural IgM antibody present in human serum. *J Immunol* **126**: 1562–1568.
8. DePolo, NJ, Reed, JD, Sheridan, PL, Townsend, K, Sauter, SL, Jolly, DJ *et al.* (2000). VSV-G pseudotyped lentiviral vector particles produced in human cells are inactivated by human serum. *Mol Ther* **2**: 218–222.
9. Baekelandt, V, Eggermont, K, Michiels, M, Nuttin, B and Debyser, Z (2003). Optimized lentiviral vector production and purification procedure prevents immune response after transduction of mouse brain. *Gene Ther* **10**: 1933–1940.
10. Hwang, BY and Schaffer, DV (2013). Engineering a serum-resistant and thermostable vesicular stomatitis virus G glycoprotein for pseudotyping retroviral and lentiviral vectors. *Gene Ther* **20**: 807–815.
11. Brown, BD, Sitia, G, Annoni, A, Hauben, E, Sergi, LS, Zingale, A *et al.* (2007). *In vivo* administration of lentiviral vectors triggers a type I interferon response that restricts hepatocyte gene transfer and promotes vector clearance. *Blood* **109**: 2797–2805.
12. Rossetti, M, Gregori, S, Hauben, E, Brown, BD, Sergi, LS, Naldini, L *et al.* (2011). HIV-1-derived lentiviral vectors directly activate plasmacytoid dendritic cells, which in turn induce the maturation of myeloid dendritic cells. *Hum Gene Ther* **22**: 177–188.
13. Gollins, SW and Porterfield, JS (1985). Flavivirus infection enhancement in macrophages: an electron microscopic study of viral cellular entry. *J Gen Virol* **66 (Pt 9)**: 1969–1982.
14. McCullough, KC, Parkinson, D and Crowther, JR (1988). Opsonization-enhanced phagocytosis of foot-and-mouth disease virus. *Immunology* **65**: 187–191.
15. Takeda, A, Tuazon, CU and Ennis, FA (1988). Antibody-enhanced infection by HIV-1 via Fc receptor-mediated entry. *Science* **242**: 580–583.
16. Jolly, PE, Huso, DL, Sheffer, D and Narayan, O (1989). Modulation of lentivirus replication by antibodies: Fc portion of immunoglobulin molecule is essential for enhancement of binding, internalization, and neutralization of visna virus in macrophages. *J Virol* **63**: 1811–1813.
17. Croyle, MA, Callahan, SM, Auricchio, A, Schumer, G, Linse, KD, Wilson, JM *et al.* (2004). PEGylation of a vesicular stomatitis virus G pseudotyped lentivirus vector prevents inactivation in serum. *J Virol* **78**: 912–921.
18. Cullis, PR, Chonn, A and Semple, SC (1998). Interactions of liposomes and lipid-based carrier systems with blood proteins: Relation to clearance behaviour in vivo. *Adv Drug Deliv Rev* **32**: 3–17.
19. Yang, L, Bailey, L, Baltimore, D and Wang, P (2006). Targeting lentiviral vectors to specific cell types in vivo. *PNAS* **26**: 326–334.
20. Wang, CX, Sather, BD, Wang, X, Adair, J, Khan, I, Singh, S *et al.* (2014). Rapamycin relieves lentiviral vector transduction resistance in human and mouse hematopoietic stem cells. *Blood* **124**: 913–923.
21. Pariente, N, Morizono, K, Virk, MS, Petrigliano, FA, Reiter, RE, Lieberman, JR *et al.* (2007). A novel dual-targeted lentiviral vector leads to specific transduction of prostate cancer bone metastases *in vivo* after systemic administration. *Mol Ther* **15**: 1973–1981.
22. Padmashali, RM and Andreadis, ST (2011). Engineering fibrinogen-binding VSV-G envelope for spatially- and cell-controlled lentivirus delivery through fibrin hydrogels. *Biomaterials* **32**: 3330–3339.
23. Frecha, C, Costa, C, Lévy, C, Nègre, D, Russell, SJ, Maisner, A *et al.* (2009). Efficient and stable transduction of resting B lymphocytes and primary chronic lymphocyte leukemia cells using measles virus gp displaying lentiviral vectors. *Blood* **114**: 3173–3180.
24. Nguyen, TH, Pagès, JC, Farge, D, Briand, P and Weber, A (1998). Amphotropic retroviral vectors displaying hepatocyte growth factor-envelope fusion proteins improve transduction efficiency of primary hepatocytes. *Hum Gene Ther* **9**: 2469–2479.
25. Brunger JM, Huynh NP, Guenther CM, Perez-Pinera P, Moutos FT, Sanchez-Adams J, Gersbach CA, Guilak F. (2014) Scaffold-mediated lentiviral transduction for functional tissue engineering of cartilage. *PNAS* **111**: E798–806.
26. Jiang, P, Lagenaur, CF and Narayanan, V (1999). Integrin-associated protein is a ligand for the P84 neural adhesion molecule. *J Biol Chem* **274**: 559–562.
27. Veillette, A, Thibaudeau, E and Latour, S (1998). High expression of inhibitory receptor SHPS-1 and its association with protein-tyrosine phosphatase SHP-1 in macrophages. *J Biol Chem* **273**: 22719–22728.
28. Tsai, RK and Discher, DE (2008). Inhibition of "self" engulfment through deactivation of myosin-II at the phagocytic synapse between human cells. *J Cell Biol* **180**: 989–1003.

29. Oldenborg, PA, Gresham, HD and Lindberg, FP (2001). CD47-signal regulatory protein alpha (SIRPalpha) regulates Fcgamma and complement receptor-mediated phagocytosis. *J Exp Med* **193**: 855–862.
30. Oldenborg, PA, Zheleznyak, A, Fang, YF, Lagenaur, CF, Gresham, HD and Lindberg, FP (2000). Role of CD47 as a marker of self on red blood cells. *Science* **288**: 2051–2054.
31. Kol, N, Shi, Y,Tsvitov, M, Barlam, D, Shneck, RZ, Kay, MS and Rousso, I (2007). A stiffness switch in human immunodeficiency virus. *Biophysical J* **92**: 1777–1783.
32. Sosale, NG, Rouhiparkouhi, T, Bradshaw, AM, Dimova, R, Lipowsky, R and Discher, DE (2015). Cell rigidity and shape override CD47's "self"-signaling in phagocytosis by hyperactivating myosin-II. *Blood* **125**: 542–552.
33. Takenaka, K, Prasolava, TK, Wang, JC, Mortin-Toth, SM, Khalouei, S, Gan, OI *et al.* (2007). Polymorphism in Sirpa modulates engraftment of human hematopoietic stem cells. *Nat Immunol* **8**: 1313–1323.
34. Subramanian, S, Boder, ET and Discher, DE (2007). Phylogenetic divergence of CD47 interactions with human signal regulatory protein alpha reveals locus of species specificity. Implications for the binding site. *J Biol Chem* **282**: 1805–1818.
35. Shultz, LD, Lyons, BL, Burzenski, LM, Gott, B, Chen, X, Chaleff, S *et al*. (2005). Human lymphoid and myeloid cell development in NOD/LtSz-scid IL2R gamma null mice engrafted with mobilized human hemopoietic stem cells. *J. Immunol* **174**: 6477–6489.
36. Hu, Z, Van Rooijen, N and Yang, YG (2005). Macrophages prevent human red blood cell reconstitution in immunodeficient mice. *Blood* **118**: 5938–5946.
37. Cross, D and Burmester, JK (2006). Gene therapy for cancer treatment: past, present and future. *Clin Med Res* **4**: 218–227.
38. Haura, EB, Sotomayor, E and Antonia, SJ (2003). Gene therapy for lung cancer. *Mol Biotechnol* **25**: 139–148.
39. Follenzi, A, Battaglia, M, Lombardo, A, Annoni, A, Roncarolo, MG and Naldini, L (2004). Targeting lentiviral vector expression to hepatocytes limits transgene-specific immune response and establishes long-term expression of human antihemophilic factor IX in mice. *Blood* **103**: 3700–3709.
40. Klein, I, Cornejo, JC, Polakos, NK, John, B, Wuensch, SA, Topham, DJ *et al.* (2007). Kupffer cell heterogeneity: functional properties of bone marrow derived and sessile hepatic macrophages. *Blood* **110**: 4077–4085.
41. Frecha, C, Lévy, C, Costa, C, Nègre, D, Amirache, F, Buckland, R *et al.* (2011). Measles virus glycoprotein-pseudotyped lentiviral vector-mediated gene transfer into quiescent lymphocytes requires binding to both SLAM and CD46 entry receptors. *J Virol* **85**: 5975–5985.
42. Lévy, C, Amirache, F, Costa, C, Frecha, C, Muller, CP, Kweder, H *et al.* (2012). Lentiviral vectors displaying modified measles virus gp overcome pre-existing immunity in in vivo-like transduction of human T and B cells. *Mol Ther* **20**: 1699–1712.
43. Naldini, L, Blömer, U, Gallay, P, Ory, D, Mulligan, R, Gage, FH *et al.* (1996). *In vivo* gene delivery and stable transduction of nondividing cells by a lentiviral vector. *Science* **272**: 263–267.
44. Mouro-Chanteloup, I, Delaunay, J, Gane, P, Nicolas, V, Johansen, M, Brown, EJ *et al.* (2003). Evidence that the red cell skeleton protein 4.2 interacts with the Rh membrane complex member CD47. *Blood* **101**: 338–344.
45. Tsai, RK, Rodriguez, PL and Discher, DE (2010). Self inhibition of phagocytosis: the affinity of 'marker of self' CD47 for SIRPalpha dictates potency of inhibition but only at low expression levels. *Blood Cells Mol Dis* **45**: 67–74.
46. Rodriguez, PL, Harada, T, Christian, DA, Pantano, DA, Tsai, RK and Discher, DE (2013). Minimal "Self" peptides that inhibit phagocytic clearance and enhance delivery of nanoparticles. *Science* **339**: 971–975.
47. Moore, MD and Hu, WS (2009). HIV-1 RNA dimerization: It takes two to tango. *AIDS Rev* **11**: 91–102.
48. Fuller, SD, Wilk, T, Gowen, BE, Kräusslich, HG and Vogt, VM (1997). Cryo-electron microscopy reveals ordered domains in the immature HIV-1 particle. *Curr Biol* **7**: 729–738.
49. Dorfman, T, Bukovsky, A, Ohagen, A, Höglund, S and Göttlinger, HG (1994). Functional domains of the capsid protein of human immunodeficiency virus type 1. *J Virol* **68**: 8180–8187.
50. Reicin, AS, Ohagen, A, Yin, L, Hoglund, S and Goff, SP (1996). The role of Gag in human immunodeficiency virus type 1 virion morphogenesis and early steps of the viral life cycle. *J Virol* **70**: 8645–8652.
51. Braslavsky, I, Hebert, B, Kartalov, E and Quake, SR (2003). Sequence information can be obtained from single DNA molecules. *Proc Natl Acad Sci USA* **100**: 3960–3964.
52. Coffman, VC and Wu, JQ (2014). Every laboratory with a fluorescence microscope should consider counting molecules. *Mol Biol Cell* **25**: 1545–1548.
53. Melikyan, GB, White, JM and Cohen, FS (1995). GPI-anchored influenza hemagglutinin induces hemifusion to both red blood cell and planar bilayer membranes. *J Cell Biol* **131**: 679–691.
54. Hinterdorfer PG, Tamm LK *et al.* (1994) Reconstitution of membrane fusion sites. A TIRFM study of influenza hemagglutinin-mediated membrane fusion. *J. Cell. Biol.* **269**: 20360–20368.
55. Bess, JW Jr, Gorelick, RJ, Bosche, WJ, Henderson, LE and Arthur, LO (1997). Microvesicles are a source of contaminating cellular proteins found in purified HIV-1 preparations. *Virology* **230**: 134–144.
56. Vintersten, K, Monetti, C, Gertsenstein, M, Zhang, P, Laszlo, L, Biechele, S *et al.* (2004). Mouse in red: red fluorescent protein expression in mouse ES cells, embryos, and adult animals. *Genesis* **40**: 241–246.
57. Bevis, BJ and Glick, BS (2002). Rapidly maturing variants of the Discosoma red fluorescent protein (DsRed). *Nat Biotechnol* **20**: 83–87.
58. Davis, HE, Morgan, JR and Yarmush, ML (2002). Polybrene increases retrovirus gene transfer efficiency by enhancing receptor-independent virus adsorption on target cell membranes. *Biophys Chem* **97**: 159–172.
59. Burns, JC, Friedmann, T, Driever, W, Burrascano, M and Yee, JK (1993). Vesicular stomatitis virus G glycoprotein pseudotyped retroviral vectors: concentration to very high titer and efficient gene transfer into mammalian and nonmammalian cells. *Proc Natl Acad Sci USA* **90**: 8033–8037.
60. Oshima, K, Ruhul Amin, AR, Suzuki, A, Hamaguchi, M and Matsuda, S (2002). SHPS-1, a multifunctional transmembrane glycoprotein. *FEBS Lett* **519**: 1–7.
61. Strowig, T, Rongvaux, A, Rathinam, C, Takizawa, H, Borsotti, C, Philbrick, W *et al.* (2011). Transgenic expression of human signal regulatory protein alpha in Rag2-/-gamma©-/- mice improves engraftment of human hematopoietic cells in humanized mice. *Proc Natl Acad Sci USA* **108**: 13218–13223.
62. Fukunaga, A, Nagai, H, Noguchi, T, Okazawa, H, Matozaki, T, Yu, X *et al.* (2004). Src homology 2 domain-containing protein tyrosine phosphatase substrate 1 regulates the migration of Langerhans cells from the epidermis to draining lymph nodes. *J Immunol* **172**: 4091–4099.
63. Finkelshtein, D, Werman, A, Novick, D, Barak, S and Rubinstein, M (2013). LDL receptor and its family members serve as the cellular receptors for vesicular stomatitis virus. *Proc Natl Acad Sci USA* **110**: 7306–7311.
64. Brown, MS, Herz, J and Goldstein, JL (1997). LDL-receptor structure. Calcium cages, acid baths and recycling receptors. *Nature* **388**: 629–630.
65. Johannsdottir, HK, Mancini, R, Kartenbeck, J, Amato, L and Helenius, A (2009). Host cell factors and functions involved in vesicular stomatitis virus entry. *J Virol* **83**: 440–453.
66. Olazabal, IM, Caron, E, May, RC, Schilling, K, Knecht, DA and Machesky, LM (2002). Rho-kinase and myosin-II control phagocytic cup formation during CR, but not FcgammaR, phagocytosis. *Curr Biol* **12**: 1413–1418.
67. Allingham, JS, Smith, R and Rayment, I (2005). The structural basis of blebbistatin inhibition and specificity for myosin II. *Nat Struct Mol Biol* **12**: 378–379.
68. Dvorak, HF, Nagy, JA, Dvorak, JT and Dvorak, AM (1988). Identification and characterization of the blood vessels of solid tumors that are leaky to circulating macromolecules. *Am J Pathol* **133**: 95–109.
69. Platt, VM and Szoka, FC Jr (2008). Anticancer therapeutics: targeting macromolecules and nanocarriers to hyaluronan or CD44, a hyaluronan receptor. *Mol Pharm* **5**: 474–486.
70. O'Connor SW, Bale WF. (1988) Accessibility of circulating IgG to extravascular compartment of rat tumors. *Cancer Res*. **44**:3348–54.
71. Wong, C, Stylianopoulos, T, Cui, J, Martin, J, Chauhan, VP, Jiang, W *et al.* (2011). Multistage nanoparticle delivery system for deep penetration into tumor tissue. *Proc Natl Acad Sci USA* **108**: 2426–2431.
72. Boyer, V, Desgranges, C, Trabaud, MA, Fischer, E and Kazatchkine, MD (1991). Complement mediates human immunodeficiency virus type 1 infection of a human T cell line in a CD4- and antibody-independent fashion. *J Exp Med* **173**: 1151–1158.
73. Offit, PA, Clark, HF, Taylor, AH, Hess, RG, Bachmann, PA and Plotkin, SA (1984). Rotavirus-specific antibodies in fetal bovine serum and commercial preparations of serum albumin. *J Clin Microbiol* **20**: 266–270.
74. Loegering, DJ, Blumenstock, FA and Cuddy, BG (1989). Determination of Kupffer cell Fc receptor function *in vivo* following injury. *Proc Soc Exp Biol Med* **192**: 255–260.
75. Montalvao, F, Garcia, Z, Celli, S, Breart, B, Deguine, J, Van Rooijen, N *et al.* (2013). The mechanism of anti-CD20-mediated B cell depletion revealed by intravital imaging. *J Clin Invest* **123**: 5098–5103.
76. Denham, S, Barfoot, R and Sills, J (1990). The rat FcR for monomeric IgG is preferentially expressed on red pulp macrophages in the spleen. *Immunology* **69**: 329–331.
77. Gardai, SJ, McPhillips, KA, Frasch, SC, Janssen, WJ, Starefeldt, A, Murphy-Ullrich, JE *et al.* (2005). Cell-surface calreticulin initiates clearance of viable or apoptotic cells through trans-activation of LRP on the phagocyte. *Cell* **123**: 321–334.
78. Majeti, R, Chao, MP, Alizadeh, AA, Pang, WW, Jaiswal, S, Gibbs, KD Jr *et al.* (2009). CD47 is an adverse prognostic factor and therapeutic antibody target on human acute myeloid leukemia stem cells. *Cell* **138**: 286–299.
79. Cameron, CM, Barrett, JW, Mann, M, Lucas, A and McFadden, G (2005). Myxoma virus M128L is expressed as a cell surface CD47-like virulence factor that contributes to the downregulation of macrophage activation in vivo. *Virology* **337**: 55–67.
80. Hatherley D, Graham SC, Turner J, Harlos K, Stuart DI, Barclay AN. (2006) Paired receptor specificity explained by structures of SIRP Alone and Complexed with CD47. *Molecular Cell* **31**:266–77.
81. Baba, N, Van, VQ, Wakahara, K, Rubio, M, Fortin, G, Panzini, B *et al.* (2013). CD47 fusion protein targets CD172a+ cells in Crohn's disease and dampens the production of IL-1β and TNF. *J Exp Med* **210**: 1251–1263.
82. Chertova, E, Bess, JW Jr, Crise, BJ, Sowder II, RC, Schaden, TM, Hilburn, JM *et al.* (2002). Envelope glycoprotein incorporation, not shedding of surface envelope glycoprotein (gp120/SU), Is the primary determinant of SU content of purified human immunodeficiency virus type 1 and simian immunodeficiency virus. *J Virol* **76**: 5315–5325.

83. Zhu, P, Chertova, E, Bess, J Jr, Lifson, JD, Arthur, LO, Liu, J *et al.* (2003). Electron tomography analysis of envelope glycoprotein trimers on HIV and simian immunodeficiency virus virions. *Proc Natl Acad Sci USA* **100**: 15812–15817.
84. Buonocore, L, Blight, KJ, Rice, CM and Rose, JK (2002). Characterization of vesicular stomatitis virus recombinants that express and incorporate high levels of hepatitis C virus glycoproteins. *J Virol* **76**: 6865–6872.
85. Navaratnarajah, CK, Leonard, VH and Cattaneo, R (2009). Measles virus glycoprotein complex assembly, receptor attachment, and cell entry. *Curr Top Microbiol Immunol* **329**: 59–76.
86. McQuaid, S and Cosby, SL (2002). An immunohistochemical study of the distribution of the measles virus receptors, CD46 and SLAM, in normal human tissues and subacute sclerosing panencephalitis. *Lab Invest* **82**: 403–409.
87. Benjamani Y and Hochberg Y. (1995) Controlling the false discovery rate: a practical and powerful approach to multiple testing. *J R Stat Soc. Series B* **57**: 298–300.

Supplementary Information accompanies this paper on the *Molecular Therapy—Methods & Clinical Development* website (http://www.nature.com/mtm)